Hydrophilic Anilinogeranyl Diphosphate Prenyl Analogues Are Ras Function Inhibitors†

Michael J. Roberts,‡ Jerry M. Troutman,‡ Kareem A. H. Chehade,‡ Hyuk C. Cha,§ Joseph P. Y. Kao,§ Xiaoqin Huang,|| Chang-Guo Zhan,|| Yuri K. Peterson,⊥ Thangaiah Subramanian,‡ Srinivasan Kamalakkannan,‡ Douglas A. Andres,‡ and H. Peter Spielmann*,‡,@

Department of Molecular and Cellular Biochemistry, Department of Chemistry, Kentucky Center for Structural Biology, and Department of Pharmaceutical Sciences, University of Kentucky, Lexington, Kentucky 40536-0084, Medical Biotechnology Center, University of Maryland Biotechnology Institute, and Department of Physiology, University of Maryland School of Medicine, Baltimore, Maryland 21201, and Department of Pharmacology and Cancer Biology, Duke University Medical Center, Durham, North Carolina 27710

Received August 21, 2006; Revised Manuscript Received November 1, 2006

ABSTRACT: Sequential processing of H-Ras by protein farnesyl transferase (FTase), Ras converting enzyme (Rce1), and protein-*S*-isoprenylcysteine *O*-methyltransferase (Icmt) to give H-Ras C-terminal farnesyl-*S*-cysteine methyl ester is required for appropriate H-Ras membrane localization and function, including activation of the mitogen-activated protein kinase (MAPK) cascade. We employed a *Xenopus laevis* oocyte whole-cell model system to examine whether anilinogeranyl diphosphate analogues of similar shape and size, but with a hydrophobicity different from that of the FTase substrate farnesyl diphosphate (FPP), could ablate biological function of H-Ras. Analysis of oocyte maturation kinetics following microinjection of in vitro analogue-modified H-Ras into isoprenoid-depleted oocytes revealed that analogues with a hydrophobicity near that of FPP supported H-Ras biological function, while the analogues *p*-nitroanilinogeranyl diphosphate (*p*-NO_2-AGPP), *p*-cyanoanilinogeranyl diphosphate (*p*-CN-AGPP), and isoxazolaminogeranyl diphosphate (Isox-GPP) with hydrophobicities 2−5 orders of magnitude lower than that of FPP did not. We found that although H-Ras modified with FPP analogues *p*-NO_2-AGPP, *p*-CN-AGPP, and Isox-GPP was an efficient substrate for C-terminal postprenylation processing by Rce1 and Icmt, co-injection of H-Ras with analogues *p*-NO_2-AGPP, *p*-CN-AGPP, or Isox-GPP could not activate MAPK. We propose that H-Ras biological function requires a minimum lipophilicity of the prenyl group to allow important interactions downstream of the C-terminal processed H-Ras protein. The hydrophilic FPP analogues *p*-NO_2-AGPP, *p*-CN-AGPP, and Isox-GPP are H-Ras function inhibitors (RFIs) and serve as lead compounds for a unique class of potential anticancer therapeutics.

A wide variety of proteins, including Ras, require post-translational prenylation for their proper membrane localization and activity (*1*−*5*). Protein farnesyltransferase (FTase)[1] catalyzes the transfer of a farnesyl group from farnesyl diphosphate (FPP, **1**, Figure 1) to proteins with a cysteine residue located in a C-terminal Ca_1a_2X motif, where C is the modified cysteine, a_1 and a_2 are often aliphatic residues, and X is Ser, Met, Ala, or Gln (*6*−*9*). Farnesylation is the first and obligatory step in an ordered series of post-translational modifications (Figure 2) that direct membrane localization and potentially protein−protein interactions for a variety of proteins involved in cellular regulatory events (*10*−*13*). After farnesylation, the a_1a_2X peptide is cleaved by the endopeptidase Rce1 (*14*, *15*) followed by methylation of the carboxyl of the now terminal farnesylated cysteine residue by protein-*S*-isoprenylcysteine *O*-methyltransferase (Icmt) (*16*). The hydrophobic moment of some of these

† This work was supported in part by the Kentucky Lung Cancer Research Program (to H.P.S. and D.A.A.) and the National Institutes of Health (Grant GM66152 to H.P.S. and Grant GM56481 to J.P.Y.K.), and the NMR instruments used in this work were obtained with support from NSF CRIF Grant CHE-9974810. Y.K.P. was supported by NIH Grant GM46372 (to P. J. Casey).

* To whom correspondence should be addressed. E-mail: hps@uky.edu. Phone: (859) 257-4790. Fax: (859) 257-8940.

‡ Department of Molecular and Cellular Biochemistry, University of Kentucky.

§ University of Maryland Biotechnology Institute and University of Maryland School of Medicine.

|| Department of Pharmaceutical Sciences, University of Kentucky.

⊥ Duke University Medical Center.

@ Department of Chemistry and Kentucky Center for Structural Biology, University of Kentucky.

[1] Abbreviations: FTase, protein farnesyltransferase; FPP, farnesyl diphosphate; GPP, geranyl diphosphate; FTI, protein farnesyltransferase inhibitor; CaaX, tetrapeptide sequence cysteine-aliphatic amino acid-aliphatic amino acid-X (serine, glutamine, or methionine for FTase); GVBD, germinal vesicle breakdown; dns, dansylated; RP-HPLC, reverse phase high-performance liquid chromatography; H-Ras, Harvey-Ras; H-RasQ61L, constitutively active H-Ras; MAPK, mitogen-activated protein kinase; AGPP, anilinogeranyl diphosphate; RFI, Ras function inhibitor; Rce1, Ras-converting enzyme 1; Icmt, protein-*S*-isoprenylcysteine *O*-methyltransferase; BME, *β*-mercaptoethanol; IPTG, isopropyl *β*-D-thiogalactopyranoside; DTT, dithiothreitol; HEPES, 4-(2-hydroxyethyl)-1-piperazineethanesulfonic acid; TCEP, tris(2-carboxyethyl)phosphine hydrochloride; SDS−PAGE, sodium dodecyl sulfate−polyacrylamide gel electrophoresis; EDTA, (ethylenedinitrilo)tetraacetic acid; EGTA, (ethylene glycol dinitrilo)tetraacetic acid; HRP, horseradish peroxidase; [^{3}H]AdoMet, *S*-adenosyl-L-methionine tritiated on the methyl group; AdoHCy, *S*-adenosyl-L-homocysteine.

10.1021/bi061704+ CCC: $33.50
Published on Web 12/06/2006

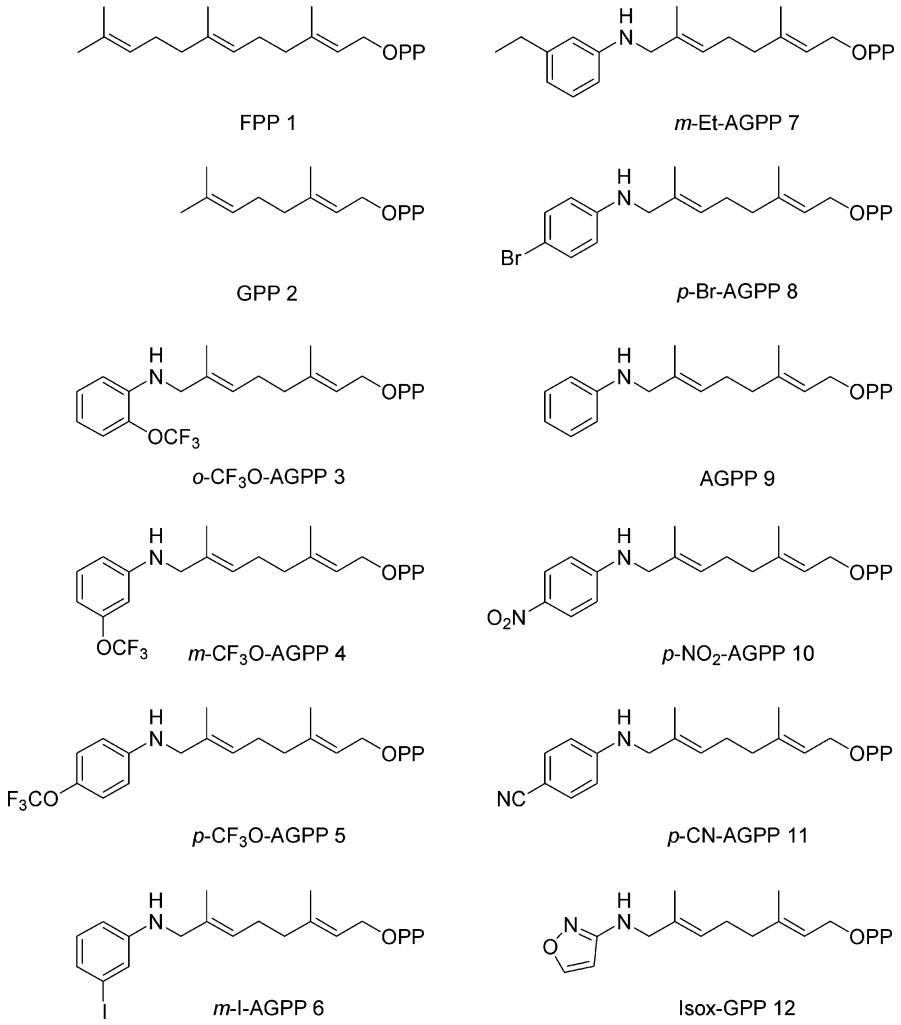

FIGURE 1: FPP and FPP analogues.

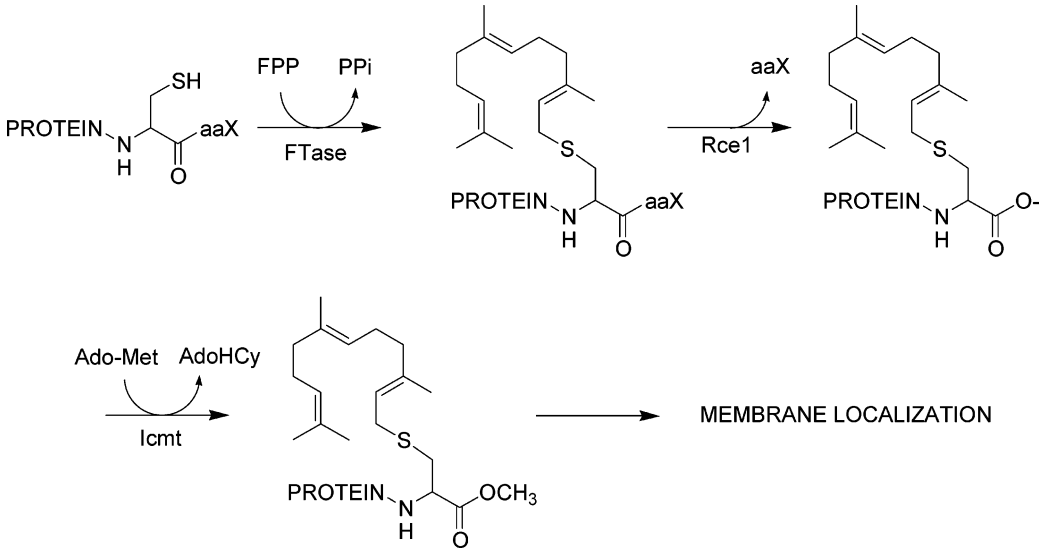

FIGURE 2: Farnesylated protein processing.

proteins is further increased by palmitoylation at one or two cysteine residues near the farnesylated C-terminus (*17*, *18*). Specifically, prenylation is obligatory for the oncogenic effects of mutant Ras (*19*). Mutated forms of Ras genes are among the most common genetic abnormalities in human cancer, occurring in 10−30% of all neoplasms (*20*−*22*). These observations have led to the development of a number of FTase inhibitors (FTIs) which block Ras farnesylation, appropriate subcellular localization, and activity, in addition to inhibiting growth of H-Ras transformed cells. Various FTIs are currently in phase I−III clinical trials as antineoplastic agents (*23*−*25*). Similar post-translational modifications occur on a diverse array of farnesylated cellular proteins, not all of which have been identified or characterized.

Interestingly, various lines of evidence suggest that one or more of these proteins, other than Ras, may serve as the actual functional target(s) of FTIs (*26*−*29*).

Farnesylation alone is insufficient for promotion of the biological function of H-Ras as the subsequent downstream steps are needed for efficient membrane localization (*30*−*33*). FTIs disrupt membrane localization by blocking the first and obligatory step in this ordered series of reactions and ablates membrane localization of H-Ras (*16*, *34*−*36*). Functional studies in *Xenopus laevis* oocytes microinjected with farnesyl analogue modified H-Ras strongly suggest that the hydrophobicity of the lipid is the most important factor in conferring Ras activity (*37*). FPP analogues stripped of most isoprenoid features such as methyl groups and unsaturation so that they more resemble simple fatty acids are transferred to Ras by FTase and allow Ras to function in a *Xenopus* signal transduction model system (*37*). H-Ras genetically engineered to become geranylgeranylated is as effective as the farnesylated molecule in supporting cell transformation (*27*).

Proteins modified with the 20-carbon geranylgeranyl group are more hydrophobic than the 15-carbon farnesyl group, and both classes of prenylated proteins are processed by Rce1 and Icmt. Replacement of the farnesyl group with FTase-transferrable lipid analogues with hydrophobicity similar or greater than that of FPP still allows all of the subsequent downstream processing events to take place (*37*). Substitution of the smaller, less hydrophobic 10-carbon geranyl group for the farnesyl group on H-Ras significantly delays the membrane association of the molecule (*37*). Importantly, it was concluded that the reduced hydrophobicity of the geranyl group impaired processing downstream of prenylation by slowing either the endoproteolysis or carboxyl methylation steps (*37*). Once processing of the C-terminus of the geranylated H-Ras was complete, normal palmitoylation followed by membrane association was observed. These observations suggest that the precise structure of the farnesyl group is not critical for the function of the protein as long as it is sufficiently hydrophobic to allow downstream processing. However, it was not possible to distinguish whether the significantly smaller size of the geranyl group impeded the processing of H-Ras by the Rce1 endoprotease and/or Icmt protein-*S*-isoprenylcysteine *O*-methyltransferase.

The observations described above suggest that FTase-catalyzed transfer of FPP analogues with significantly different structures, or with hydrophobicity lower than that of GPP (**2**), may completely block the membrane localization of H-Ras by preventing downstream processing of the alternatively modified C-terminus. This view suggests that an attractive alternative to inhibition of FTase by FTIs is disruption of cellular functions through FTase-catalyzed incorporation of unnatural farnesyl analogues into proteins that are normally farnesylated (*38*). Distinguishing the effects of lipid hydrophobicity and size requires the evaluation of additional, structurally diverse, farnesyl analogues for development of a structure−activity relationship for the lipid.

The *X. laevis* oocyte is a convenient in vitro system for studying farnesylation-dependent cellular signal transduction (*31*, *37*). Oocytes are naturally arrested at the G2−M boundary of the first meiotic cell division (*37*). Microinjection of bacterially expressed, oncogenic H-Ras (H-RasQ61L) promotes the meiotic maturation in a process accompanied by activation of mitogen-activated protein kinase (MAPK) (*31*, *37*, *39*). Because bacteria lack the enzymes required for protein isoprenylation and subsequent processing, the ability of recombinant H-Ras to induce meiotic maturation is completely dependent on intracellular farnesylation of the protein (*40*). Therefore, depletion of the endogenous pool of isoprenoids by treatment of the oocytes with inhibitors of 3-hydroxy-3-methylglutaryl-CoA reductase (HMG-CoA reductase), such as lovastatin, blocks the ability of bacterially expressed H-Ras to induce maturation. Microinjection of H-Ras modified in vitro by FTase with FPP analogues into *X. laevis* oocytes allows the biological signal transduction functions of the lipidated protein to be studied (*37*, *41*).

Table 1: Physical Properties of Isoprenoids

isoprenoid	logP[a]	surface area difference relative to farnesol **1** (Å^2)[b]
1, FPP	6.1	0
2, GPP	3.6	−79
3, *o*-CF_3O-AGPP	5.1	30
4, *m*-CF_3O-AGPP	4.9	41
5, *p*-CF_3O-AGPP	4.9	42
6, *m*-I-AGPP	4.8	35
7, *m*-Et-AGPP	4.6	39
8, *p*-Br-AGPP	4.6	27
9, AGPP	3.6	4
10, *p*-NO_2-AGPP	3.1	25
11, *p*-CN-AGPP	2.9	21
12, Isox-GPP	0.7	−1

[a] LogP measurements of the corresponding alcohol. [b] The surface area of alcohol refers to the solvent accessible surface, determined using a probe radius of 1.4 Å, and calculated as the difference relative to farnesol. The surface area of farnesol is 276 Å^2.

We have prepared a series of FPP analogues (**3**−**12**) with molecular surface areas and shapes similar to those of FPP but with a wide range of lipophilicities (Figure 1 and Table 1). The wide range of lipophilicity spanned by these structures is indicated by the logP of the parent alcohols. LogP, the logarithm of the partition coefficient between water-saturated octanol and octanol-saturated water, is a useful metric of the ability of compounds to associate with membranes. The unnatural anilinogeranyl diphosphate analogues **3**−**12** (Figure 1) are alternative substrates for mammalian FTase and have structures and physical properties quite different from those of FPP **1**. We also show that H-Ras modified with unnatural analogues AGPP **9**, *p*-NO_2-AGPP **10**, *p*-CN-AGPP **11**, and Isox-GPP **12** were processed by Rce1 and Icmt as efficiently as H-Ras modified with FPP, while H-Ras modified with the smaller GPP **2** was much less efficiently processed. Utilizing the *X. laevis* oocyte system, we find that H-Ras modified with hydrophobic anilinogeranyl diphosphate derivatives **4**−**9** supports H-Ras-dependent maturation and activation of mitogen-activated protein kinase, while more hydrophilic derivatives *p*-NO_2-AGPP **10**, *p*-CN-AGPP **11**, and Isox-GPP **12** prevent this Ras-dependent maturation. With the suite of FPP analogues **3**−**12** used in this study, we were able to separate the effect of lipid size from hydrophobicity in the H-Ras-stimulated maturation of oocytes. These results suggest that whereas analogues **4**−**12** all support full processing of the H-Ras C-terminus by FTase, Rce1, and Icmt, the more hydrophilic FPP analogues (*p*-NO_2-AGPP **10**, *p*-CN-AGPP **11**, and Isox-GPP **12**) are Ras function inhibitors (RFIs) and serve as lead

compounds for a unique class of potential anticancer therapeutics.

EXPERIMENTAL PROCEDURES

Farnesyl Diphosphate Analogues. Analogues **3**−**12** were prepared on solid support or in solution as previously described by Subramanian et al. (*42*) and Chehade et al. (*43*). FPP **1** and GPP **2** were synthesized as described by Davisson et al. (*44*). Full details of the organic synthesis and spectroscopic characterization of new compounds **6**, **7**, **11**, and **12** are provided as Supporting Information.

$k_{cat}/K_m^{peptide}$ Determination. The kinetic constant $k_{cat}/K_m^{peptide}$ for transfer of isoprenoids **1**−**12** by FTase to peptide was determined using a continuous spectrofluorometric assay originally developed by Pompliano et al. (*45*) and modified for a 96-well plate format. Utilizing *N*-dansyl-GCVLS (Peptidogenics) as the peptide substrate, we measured the linear portion of the increase in fluorescence versus time with a SpectraMax GEMINI XPS microplate reader (excitation wavelength, 340 nm; emission wavelength, 505 nm with a 10 nm cutoff). Each assay in a total volume of 300 μL containing 50 mM Tris-HCl (pH 7.4), 12 mM $MgCl_2$, 12 μM $ZnCl_2$, 0.0167% *n*-dodecyl β-D-maltoside (DM), 6.7 mM DTT, 6.7 μM isoprenoid diphosphate (FPP or AGPP from a 25 mM NH_4HCO_3 stock solution to give a final NH_4HCO_3 concentration of 0.8 mM), and *N*-dansyl-GCVLS peptide (variable concentrations; see below) was assembled in individual wells of a black, flat-bottom, polystyrene 96-well plate with nonbinding surface (Corning). The plate was then incubated at 30 °C for 20 min. The reaction was then initiated by addition of FTase (final concentration of 5 nM for analogues **1**, **4**−**6**, and **8**−**11** and 20 nM for analogues **2**, **7**, and **12**), and fluorescence was measured at 30 °C for 60 min. Each FPP analogue was assayed in triplicate wells. Peptide concentrations for determining $K_m^{peptide}$ were chosen on the basis of $K_m^{peptide}$ estimates from reactions with 0.5, 1, 5, and 10 μM *N*-dansyl-GCVLS concentrations. In the final analysis, eight peptide concentrations were used, corresponding approximately to 0.17, 0.2, 0.25, 0.5, 0.75, 1, 2, and 3 times the estimated $K_m^{peptide}$ value. The velocity of each reaction was determined by converting the rate of the increase in fluorescence intensity units (FLU/s) to micromolar per second (μM/s) by fitting the data to eq 1

$$V = (RP)/(F_{max} - F_{min}) \quad (1)$$

where V is the velocity of the reaction in μM/s, R is the rate of the reaction in FLU/s, P is the concentration of modified product in micromolar (see below), F_{max} is the fluorescence intensity of the fully modified product, and F_{min} is the fluorescence of a reaction mixture to which 5 μL of assay buffer was added in place of FTase. HPLC analysis was used to confirm complete modification of peptides after the fluorescence of a reaction mixture stabilized for more than 10 min (see below). The fluorescence of a few reaction mixtures that contained higher concentrations of peptide increased continuously over the time period of the assay. For these samples, the value for $F_{max} - F_{min}$ was estimated by linear extrapolation from a plot of $F_{max} - F_{min}$ versus peptide concentration for reactions that had gone to completion.

The velocities of the reactions were plotted against the concentration of peptide and then fit to the Michaelis−Menten equation (eq 2) to give the apparent k_{cat} and $K_m^{peptide}$ values. Due to peptide substrate inhibition, only initial velocity data from peptide concentrations that gave an error of <20% in the nonlinear fit of eq 2 were included in the analysis.

$$V/E_t = (k_{cat}[Pep])/(K_m^{peptide} + [Pep]) \quad (2)$$

where E_t is the total enzyme concentration and [Pep] is the total input peptide concentration.

Product Studies. Reactions were prepared as described above and stopped after 1 h by addition of 50 μL of isopropyl alcohol and acetic acid (8:2). The plate was then placed in a HPLC system (Agilent 1100) equipped with a microplate autosampler, a fluorescence detector, and a diode array detector. One hundred microliters of the reaction mixture was loaded onto an analytical C18 column (Microsorb, Varian) and eluted with a linear gradient from 10 to 100% CH_3CN in water over 20 min; the eluant contained 0.01% (v/v) TFA. Analogue-modified peptides had longer retention times than the corresponding unmodified peptides due to an increase in hydrophobicity.

LogP Determination. The apparent logP values for the corresponding alcohols for compounds **1**−**12** were estimated from the capacity factors (k') using reverse phase high-performance liquid chromatography (RP-HPLC) (*46*, *47*). A BioBasic-8 RP-C8 column was used as the stationary phase, and the mobile phase consisted of a mixture of 20 mM phosphate buffer (pH 6.0) and methanol (3:7) as described by Niemi et al. (*47*). Solutions with known logP values were prepared in 3:7 phosphate buffer in methanol [1 mM progesterone (logP = 3.87), 1 mM norgestrel (logP = 3.7), 100 mM anthracene (logP = 4.54), 1 mM hydrocortisone (logP = 1.53), 0.01 mM nitrobenzene (logP = 1.85), 0.01 mM anisole (logP = 2.11), 1 mM perylene (logP = 6.25), and 0.05 mM naphthalene (logP = 3.3)]. Five microliters of each standard was injected and monitored at 254 and 280 nm. A standard curve was generated from the log of the capacity factor, k', calculated with eq 3

$$k' = (R_t - R_0)/R_0 \quad (3)$$

where R_t is the retention time and R_0 is the time for a 5 μL injection of 1 mM benzoic acid to pass through the column. The log k' was plotted against the known logP values to generate a standard curve ($R^2 > 0.9$). The apparent logP for parent alcohols **1**−**12** was determined by comparing each log k' value against the standard curve.

Surface Area Calculation. Surface areas of the lipid portions of analogues **1**−**12** were estimated using a molecular modeling approach. Initial molecular structures of the compounds considered in this study were built by using Sybyl 7.0 (*48*) on an SGI Fuel workstation. The structures were energy-minimized by using a molecular mechanics method with the Tripos force field and Gasteiger−Hückel charges (*49*). When Gasteiger−Hückel charges were generated, the net charge was assigned to be 0 for each alcohol and −3.0e for each diphosphate form. A nonbond cutoff of 8 Å was used in the energy minimization to account for the intramolecular interactions. The energy minimization (i.e.,

the full geometry optimization) was carried out until the convergence criterion of 0.01 kcal mol^{-1} $Å^{-1}$ was achieved. The energy-minimized molecular structures were employed to calculate the van der Waals molecular surfaces and the solvent accessible surface area (SASA) by using WebLab Viewpro (*50*). In the SASA calculations, a probe atom with a radius of 1.4 Å was used.

H-Ras Protein. Oncogenic H-RasQ61L was expressed in the Rosetta DE3 strain of *Escherichia coli* (Novagen) using the pTrc-His A plasmid (Invitrogen). Expression was induced with 1 mM isopropyl β-D-thiogalactopyranoside (IPTG) when the optical density of the bacterial culture reached 0.6, and the bacteria were harvested after 4 h (*51*). Bacteria were pelleted by centrifugation, resuspended in 20 mM Tris (pH 8.0) containing 0.5 M NaCl, 1 mM BME, 1 mM $MgCl_2$, 10% glycerol, and 20 mM imidazole, and lysed using a French press, and H-RasQ61L was purified on a nickel column by fast protein liquid chromatography using an imidazole gradient. Aliquots from the resulting fractions were separated on a 12% SDS−PAGE gel, which was then stained by being incubated with Coomassie Blue (0.625 g in 250 mL of 50% MeOH and 10% acetic acid) for 1 h followed by destaining (3:1 MeOH/acetic acid mixture). Fractions shown to contain pure (>90%) H-RasQ61L by SDS−PAGE were dialyzed against Tris. Protein concentrations were measured using the BCA protein assay kit (Pierce), and this value was used in subsequent experiments.

Premodification of H-Ras in Vitro Using FPP Analogues. H-RasQ61L (100 μM) was incubated in assay buffer (52 mM Tris-HCl, 12 mM $MgCl_2$, 12 μM $ZnCl_2$, and 5.8 mM DTT), with 100 μM FPP or FPP analogues (**1**−**12**), 1 μM recombinant FTase, and 0.04% *n*-dodecyl β-D-maltoside in a total volume of 15 μL for 20 min at 37 °C (*43*). The reaction mixture containing the lipidated H-RasQ61L was then immediately injected into lovastatin-treated oocytes as described below.

Oocyte Extraction and Microinjection. Oocytes were isolated from *X. laevis* females (Xenopus Express, Inc.) that were primed with gonadotropin before shipment and allowed to acclimatize to their new environment for a minimum of 30 days after arrival before surgery. Frogs were housed in water tanks maintained at 17 °C and given a 12 h−12 h light−dark cycle for optimal egg production. After the frogs were anesthetized with 0.01% MS-222 (Argent), the oocytes were surgically removed; the frogs were then returned to the communal tank for recovery. Oocytes were defoliculated by incubation with 3 mg/mL type 3 collagenase (Worthington Chemical Corp.), in 30 mL of Barth's medium [88 mM NaCl, 1 mM KCl, 2.4 mM $NaHCO_3$, 0.82 mM $MgSO_4$, 0.33 mM $Ca(NO_3)_2$, 0.41 mM $CaCl_2$, and 20 mM HEPES (pH 7.5)], for 60−90 min. Following defoliculation, oocytes were washed three times in Barth's medium (30 mL each time) and three times in one-half Leibowitz L15 medium (Invitrogen) (30 mL each time) and allowed to recover for at least 4 h before being used. Following recovery, stage V and VI oocytes were selected and incubated overnight (16 h) in one-half L15 medium with or without 50 μM lovastatin (LKT Laboratories). Following incubation, any oocytes that were not of uniform pigmentation and otherwise healthy were discarded; the remaining oocytes were microinjected with H-RasQ61L premodified as described above, or H-RasQ61L was co-injected with the FPP analogues (*42*, *52*). The total volume of injection was 50 nL/oocyte. All microinjections were conducted using a Nanoject II microinjector (Drummond Scientific Co.) mounted on a micromanipulator (Narishige). Oocytes were scored hourly for germinal vesicle breakdown (GVBD), as evidenced by the appearance of a white spot in the otherwise dark-colored animal hemisphere. Progesterone was used as a positive control to induce GVBD in lovastatin-treated and untreated oocytes and to determine whether any oocytes that did not undergo GVBD following microinjection of the FPP analogues were still responsive to maturation signals.

Gel Shift Assay. Following modification of H-Ras for exactly 20 min as described above, a 1 μL sample was taken and immediately mixed with 4 μL of 2× Laemmli SDS sample buffer. Samples were boiled for 5 min and then loaded onto 12% SDS−PAGE gels to separate modified H-Ras from unmodified H-Ras by running at 200 V for 80 min. Proteins were stained by incubation with Coomassie Blue (0.625 g in 250 mL of 50% MeOH and 10% acetic acid) for 1 h followed by destaining (3:1 MeOH/acetic acid mixture). H-Ras modified with a prenyl group shows an electrophoretic mobility higher than that of unmodified H-Ras. The extent of protein modification by each analogue was estimated from images of the gel analyzed using NIH Image 1.63.

MAPK Activation Assay. Following microinjection, five oocytes were removed at random at appropriate time points, flash-frozen in liquid nitrogen, and stored at −80 °C until assay. Immediately before the assay, oocytes were resuspended in 50 μL of buffer containing 20 mM HEPES (pH 7.4), 50 mM β-glycerophosphate, 2 mM EGTA, 50 mM KF, 1 mM NaF, 1% Triton X-100, 10% glycerol, and 150 mM NaCl with 1 mM Na_3VO_4 and protease inhibitor cocktail (CalBiochem, San Diego, CA). Oocyte suspensions were homogenized by pipetting 15−20 times through a P200 pipet tip, vortexed, and allowed to sit on ice for 20 min. Insoluble matter was pelleted by centrifugation at 12000*g* for 15 min. The clear supernatant was resolved on a 10% SDS−PAGE gel at a loading of 0.1 oocyte equivalent per lane. Proteins were transferred to nitrocellulose, and the membranes were blocked in PCT [10 mM phosphate (pH 7.4), 150 mM NaCl, 0.1% Tween 20, and 1% casein] for at least 1 h. Activated MAPK and total MAPK were detected by incubating the membrane with primary p-ERK (E-4) antibody (Santa Cruz Biotechnology) or anti-MAPK/ERK1/2-CT antibody, respectively, in PCT for 1 h. After three 15 min washes in PT [10 mM phosphate (pH 7.4), 150 mM NaCl, and 0.1% Tween 20], the membrane was incubated with secondary anti-mouse HRP-conjugated antibody (Zymed, San Francisco, CA) for 1 h in PCT. The membrane was washed three more times in PT and developed using enhanced ECL (Supersignal, Pierce, Rockford, IL).

Data Analysis. The results are presented as means ± the standard deviation of at least three independent experiments. Through Prizm (Graphpad Software, San Diego, CA), the sigmoid curve $y = (1 + 10^{t_{1/2}-t})^{-1}$ was fit to the data.

Prenyl-Protein Protease/Methyltransferase Coupled Assay. The assay was performed with modifications to methods previously described (*14*, *15*). Briefly, protease reactions were initiated by the addition of 1 μg of Sf9 membranes containing the recombinant prenyl protein protease Rce1 to an assay mixture containing 20 nM prenylated proteins in

Table 2: In Vitro Modification of H-Ras with Isoprenoids

isoprenoid	% H-Ras modified in the in vitro reaction for microinjection[a]	$k_{cat}/K_m^{peptide}$ ($s^{-1}\,\mu M^{-1}$)[b]
1, FPP	>90	0.18 ± 0.03
2, GPP	70	0.015 ± 0.007
3, *o*-CF_3O-AGPP	0	nd[c]
4, *m*-CF_3O-AGPP	>90	0.19 ± 0.01
5, *p*-CF_3O-AGPP	>90	0.087 ± 0.003
6, *m*-I-AGPP	>90	0.26 ± 0.03
7, *m*-Et-AGPP	70	0.021 ± 0.005
8, *p*-Br-AGPP	>90	0.16 ± 0.02
9, AGPP	>90	0.24 ± 0.06
10, *p*-NO_2-AGPP	>90	0.107 ± 0.002
11, *p*-CN-AGPP	>90	0.068 ± 0.001
12, Isox-GPP	50	0.028 ± 0.002

[a] The extent of H-Ras lipidation was estimated from images of SDS−PAGE separations of in vitro FTase reaction mixtures. [b] $k_{cat}/K_m^{peptide}$ was determined using a Michaelis−Menten analysis described in Experimental Procedures. [c] Not detected.

70 mM HEPES (pH 7.4), 5 mM $MgCl_2$, and 20 mM NaCl in a total volume of 100 μL. Proteolysis reactions were conducted for 1 h at 30 °C. Following the proteolysis reaction, methylation of proteolyzed prenylated protein was initiated by addition of 2 μg of membranes containing recombinant Icmt and 200 nM [^{3}H]AdoMet (63.6 Ci/mmol) to the reaction mixture, which was then incubated for 1 h at 30 °C. Reactions were terminated by precipitation using 0.5 mL of 4% SDS, 50 μg of bovine brain cytosol as a carrier protein, and 0.5 mL of 30% TCA. ^{3}H-methylated protein was then quantified using a filter assay and liquid scintillation counting.

RESULTS

FTase-Catalyzed in Vitro Modification of H-Ras with FPP Analogues. The physical properties and kinetics of in vitro FTase-catalyzed transfer of the FPP analogues to peptide substrate depend on the structure of the analogues. Table 1 lists some of the relevant physical properties of the analogues and the isoprenoids FPP **1** and GPP **2**. With the important exception of *o*-CF_3O-AGPP **3**, all of the analogues can be transferred in vitro by recombinant rat FTase to the H-Ras CVLS Ca_1a_2X motif. The specificity constant $k_{cat}/K_m^{peptide}$ for transferring each analogue to H-Ras by FTase was within a factor of 9 of that of FPP **1** (Table 2). The apparent logP (logP^{app}) of the analogues based on HPLC capacity factors ranges from 6.1 for the lipophilic farnesyl group **1** to 0.7 for the more hydrophilic isoxazole derivative Isox-GPP **12**. Incorporation of aromatic rings and heteroatoms into the analogues decreases their hydrophobicity relative to hydrocarbons of the same size. As a result, the size and hydrophobicity of the analogues are no longer directly related. FPP **1** and AGPP **9** are almost identical in size but differ substantially in hydrophobicity. On the other hand, both the 10-carbon geranyl group of GPP **2** and the anilinogeranyl group of AGPP **9** have a logP of 3.6, near the middle of the range, but differ in surface area by 135 Å^2. Analogues **3**−**11** have a surface area up to 15% larger than that of the farnesyl moiety, while analogue Isox-GPP **12** has a surface area 7% smaller than that of the farnesyl moiety. However, the decrease in the lipophilicity of GPP **2** is accompanied by a surface area 40% smaller than that of FPP. Additionally, a variety of meta and para substituents on the aniline ring were included to test whether the biological function of H-Ras was sensitive to both the structure and hydrophobicity of the analogue.

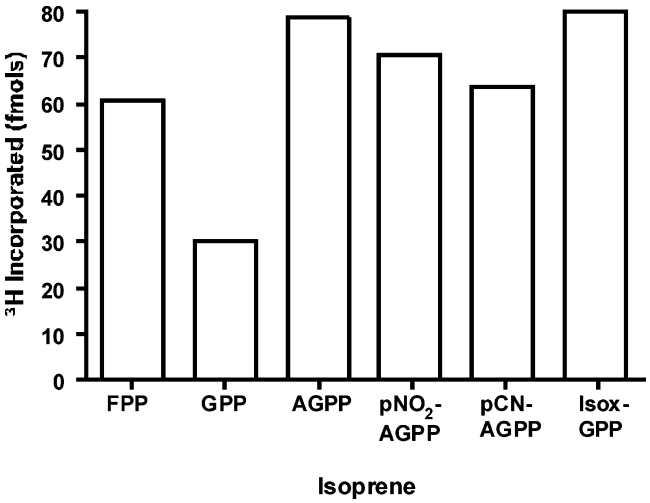

FIGURE 3: Isoprenylated Ras proteins support post-translational modification by Rce1 and Icmt. Rce1 proteolysis and subsequent Icmt methylation were assessed for Ras proteins modified with individual isoprene groups as described in Experimental Procedures. Data are expressed as the specific incorporation of each sample obtained by subtracting the incorporation into unprenylated Ras controls. Data represent the means of duplicates from a single experiment and are representative of triplicate experiments.

H-Ras Modified with Unnatural Analogues Supports Rce1 and Icmt Processing. A subset of the transferrable analogues were examined for their ability to support postprenylation proteolysis by Rce1 and methylation by Icmt. H-Ras requires postprenylation proteolysis by Rce1 and methylation by Icmt to give the mature protein with a C-terminal isoprenylcysteine methyl ester. To determine whether analogue-modified H-Ras proteins can undergo these post-translational modifications, the proteins were tested in an in vitro coupled enzyme assay. This assay takes advantage of the fact that Icmt uses only substrates bearing a C-terminal prenylated cysteine. That is, Icmt will catalyze methylation of isoprenylated H-Ras only after proteolysis by Rce1 has generated a C-terminal prenylcysteine. As shown in Figure 3, H-Ras modified with FPP **1**, GPP **2**, and analogues AGPP **9**, *p*-NO_2-AGPP **10**, *p*-CN-AGPP **11**, and Isox-GPP **12** was found to be methylated in the coupled enzyme assay, demonstrating that each of the novel isoprenoids that was tested supports proteolysis by Rce1 and subsequent methylation by Icmt. Note that H-Ras modified with GPP **2** is a significantly inferior substrate for the coupled assay compared with FPP **1** and the other analogues that were tested.

H-Ras Biological Function Depends on Prenyl Analogue Hydrophobicity, and Hydrophilic Analogues Are H-Ras Function Inhibitors. To evaluate the effect of the lipid physical properties on H-Ras function, we prepared H-Ras modified in vitro with FPP **1**, GPP **2**, and analogues **4**−**12** shown in Figure 1 for microinjection into oocytes. The extent of H-Ras modification for each analogue is given in Table 2. Lipidated H-Ras is somewhat unstable in solution, forming aggregates and precipitates upon standing for very short periods. The rate and extent of aggregation are dependent on the lipid analogue structure. In particular, in vitro modification of H-Ras with *p*-Br-AGPP **8** results in complete denaturation of the H-Ras within 5 min of initiation of the

FTase reaction. The aggregated H-Ras was clearly visible in the microinjection needle under the microscope. Except for the *p*-Br-AGPP **8**, aggregation could be controlled by allowing no more than 20 min to elapse from initiation of H-Ras lipidation to completion of oocyte microinjection. Previous studies employed detergent to keep lipidated H-Ras in solution. In our hands, the use of sufficient detergent to prevent aggregation of the anilinogeranyl analogue-modified H-Ras resulted in inconsistent oocyte maturation results.

Lovastatin-treated oocytes were microinjected with 5 pmol of in vitro analogue-modified H-Ras and scored for germinal vesicle breakdown (GVBD) over the subsequent 24−48 h period. Microinjection of H-Ras premodified with the lipid analogues ensured that the intracellular behavior was not dependent on the ability of endogenous FTase to effectively transfer the analogues. The effective dose of analogue-modified H-Ras microinjected into each oocyte was greater than 4.5 pmol each for FPP **1**, analogues **4**−**6**, and **9**−**11** but only 2.5 pmol for Isox-GPP **12** and 3.5 pmol for *m*-Et-AGPP **7** and GPP **2** due to incomplete lipidation (Table 2). The time required for 50% maturation of the oocytes was calculated from sigmoidal curves fitted to the GVBD time course for each of the analogues (Figure 4). FPP **1**, GPP **2**, and analogues **4**−**7** and AGPP **9** stimulated GVBD, while analogues *o*-CF_3O-AGPP **3**, *p*-NO_2-AGPP **10**, *p*-CN-AGPP **11**, and Isox-GPP **12** did not. Relative to FPP **1**, GVBD was delayed for analogues **4**−**7**, GPP **2**, and AGPP **9** (Table 3). Farnesylated H-Ras is the natural substrate for the downstream maturation steps and is expected to undergo efficient processing and appropriate membrane localization in the oocyte. The time required for maturation of 50% of the oocytes injected with farnesylated H-Ras ($t_{1/2}$) was highly dependent on the frog from which they were harvested. The value of $t_{1/2}$ varied from 4 to 10 h for different batches of oocytes stimulated by farnesylated H-Ras. Accordingly, individual experiments were conducted with oocytes simultaneously harvested from a single frog. We found that the order in which the analogue-modified H-Ras stimulated 50% maturation relative to farnesylated H-Ras was essentially identical from experiment to experiment. This observation gave us confidence to combine and analyze data obtained from experiments using oocytes from multiple frogs after appropriate normalization. We characterize each analogue by the ratio of its $t_{1/2}$ to that of FPP, i.e., $t_{1/2}$(analogue)/$t_{1/2}$(FPP) (Table 3). The time course of a representative oocyte maturation experiment is shown in Figure 4A.

The 5 pmol/oocyte dose of modified H-Ras is in excess of that required to achieve maximal rates of oocyte maturation. Previous studies of prenyl function showed that 2 pmol/cell of farnesylated H-Ras caused maturation at maximal rates (*37*). At the submaximal dose of 0.5 pmol/cell of modified H-Ras, the oocyte system is very sensitive to structural alterations of the lipid, which affect its biological activity. For example, microinjection of 0.5 pmol of geranyl-modified H-Ras resulted in a maturation $t_{1/2}$ that was 2.5−3.3 times longer than the $t_{1/2}$ for farnesyl-modified H-Ras (*37*). The increase in maturation time is closely associated with delays in the downstream endoproteolysis, carboxyl methylation, and subsequent palmitoylation (*37*). In contrast, the maturation of oocytes microinjected with 5 pmol/cell of 70% lipidated geranyl H-Ras (3.5 pmol of modified protein) is only delayed by 40% relative to that of farnesylated H-Ras

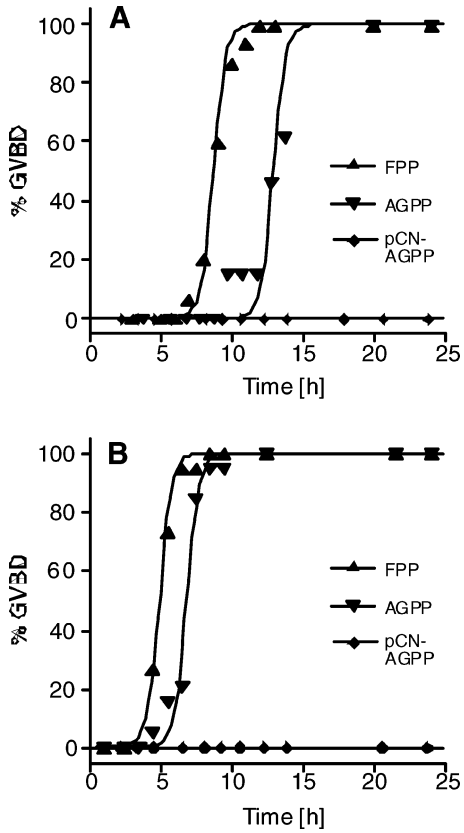

FIGURE 4: Representative kinetics of oocyte maturation induced by H-RasQ61L and FPP, AGPP, or *p*-CN-AGPP. Stage V or VI oocytes were incubated with lovastatin for 16 h and then microinjected as described in Experimental Procedures. Microinjected oocytes were monitored for GVBD at the indicated times, and the results are expressed as a percentage of the total number of viable injected oocytes (14−20 per group). (A) Induction of GVBD following microinjection of premodified activated H-Ras into lovastatin-treated oocytes. The $t_{1/2}$ was 8.8 h for farnesylated H-Ras and 13 h for anilinogeranylated H-Ras. The ratio of $t_{1/2}$(AGPP) to $t_{1/2}$(FPP) is 1.5. (B) Induction of GVBD following co-microinjection of activated H-Ras and isoprenoid diphosphate into lovastatin-treated oocytes. The $t_{1/2}$ was 5 h for FPP and 6.9 h for AGPP co-injected with H-Ras. The ratio of $t_{1/2}$(AGPP) to $t_{1/2}$(FPP) is 1.4. Oocytes microinjected with *p*-CN-anilinogeranylated H-Ras or co-microinjected with activated H-Ras and *p*-CN-AGPP failed to mature during the course of the experiment.

(Table 3). Thus, a large H-Ras dose can reveal any signal transduction activity, expressed as GVBD, that is supported by the analogues. Therefore, lipid analogues that do not support GVBD in oocytes microinjected with these large doses of modified H-Ras are extremely compromised in their ability to support oncogenic H-Ras function.

In each experiment, unmodified H-Ras was injected into both lovastatin-treated and untreated oocytes to test for the completeness of the isoprenoid depletion and as an additional check on the quality of the oocytes. As previously reported, untreated oocytes injected with activated H-Ras underwent GVBD, whereas those preincubated with lovastatin failed to mature. Progesterone stimulates GVBD via an H-Ras-independent pathway and is therefore unaffected by lovastatin treatment (*53*). In each experiment, a small number of the oocytes injected with the analogue-modified H-Ras were withheld and treated with progesterone to test the overall oocyte quality and to ensure that the manipulations did not interfere with maturation. In all cases, the progesterone-treated oocytes matured.

Table 3: Maturation Kinetics of Microinjected Oocytes

isoprenoid	fold increase in maturation time relative to that of FPP **1**[a]: in vitro modified H-Ras	fold increase in maturation time relative to that of FPP **1**[a]: co-injected H-Ras and analogue
1, FPP	1	1
2, GPP	1.4 ± 0.3	1.7 ± 0.2
3, *o*-CF_3O-AGPP	nd[b]	nd[b]
4, *m*-CF_3O-AGPP	1.6 ± 0.3	2.0 ± 0.8
5, *p*-CF_3O-AGPP	1.3 ± 0.2	1.7 ± 0.3
6, *m*-I-AGPP	1.6 ± 0.3	1.0 ± 0.1
7, *m*-Et-AGPP	1.2 ± 0.1	3.3 ± 1.0
8, *p*-Br-AGPP	no assay[c]	1.4 ± 0.2
9, AGPP	1.6 ± 0.5	1.5 ± 0.3
10, *p*-NO_2-AGPP	nd[b]	nd[b]
11, *p*-CN-AGPP	nd[b]	nd[b]
12, Isox-GPP	nd[b]	nd[b]

[a] Reported values are based on at least three independent experiments. [b] Not detected. [c] Precipitation of in vitro lipidated protein precluded a microinjection assay.

Table 3 shows that the abilities of the analogues to support oocyte maturation fall into four categories. The first category is represented by analogue *o*-CF_3O-AGPP **3**, which does not support oocyte maturation because it is not transferred to H-Ras by FTase. The second category is represented by GPP **2**, which is transferred to H-Ras and shows delays in Rce1 and/or Icmt processing (Tables 2 and 3 and Figure 3) (*37*). The third category consists of analogues **4**−**7** and AGPP **9**, which are transferred by FTase to H-Ras in vitro and support GVBD. Interestingly, the $t_{1/2}$ for maturation stimulated by these analogues was lengthened by 20−60% relative to that of farnesylated H-Ras even though AGPP **9** is efficiently processed by both Rce1 and Icmt. With respect to FPP, the increase in $t_{1/2}$ for these analogues is significant. However, the $t_{1/2}$ differences among GPP **2** and analogues **4**−**7** and AGPP **9** are not significant. The fourth category consists of analogues *p*-NO_2-AGPP **10**, *p*-CN-AGPP **11**, and Isox-GPP **12**, which are transferred by FTase to H-Ras and are efficiently processed by Rce1 and Icmt in vitro but do not support GVBD. These analogues are H-Ras function inhibitors (RFIs).

The lipid chains of FPP **1** and transferrable analogues **4**−**12** are similar in length, size, and excluded volume but have different hydrophobicities (Table 1). The delay in oocyte maturation kinetics does not show any correlation with the length or surface area of the lipid moiety. Rather, it appears that H-Ras is capable of initiating GVBD if the lipid alcohol has a logP of at least 3.6. However, H-Ras modified with lipids with a logP of <3.1 is incompetent in initiating GVBD.

In Situ Lipidation of H-Ras by Hydrophobic FPP Analogues Rescues H-Ras Biological Function in X. laevis Oocytes. The loss of H-Ras function in the experiments described above is independent of differences in the rates at which the analogues are transferred by FTase. However, partial loss of the in vitro lipidated H-Ras to aggregation was inevitable and prevented evaluation of the *p*-Br-AGPP **8** analogue. The possibility existed that different substitution patterns on the analogue might affect the ability of the lipid to support oocyte maturation. Analogues *m*-Et-AGPP **7** and *p*-Br-AGPP **8** have the same logP and have similar surface areas and excluded volumes. However, they differ in structure, with analogue *m*-Et-AGPP **7** bearing a *m*-ethyl group and analogue *p*-Br-AGPP **8** with a *p*-bromo substituent on the aniline ring. Previous studies showed that the *X. laevis* FTase could transfer lipids with hydrophobicity similar to, or greater than, that of FPP to H-Ras in situ (*37*). The rate of transfer was sufficiently high that H-Ras co-injected with lipid showed the same maturation $t_{1/2}$ as H-Ras that was modified in vitro. These results suggest that the substrate specificity of *X. laevis* FTase is sufficiently similar to that of mammalian FTase to allow efficient modification of the H-Ras by structurally unrelated analogues of FPP.

We co-injected 5 pmol each of lipid diphosphates **1**−**12** and H-Ras into lovastatin-treated oocytes and scored for GVBD. The time course of a representative oocyte maturation experiment is shown in Figure 4B, and oocyte maturation $t_{1/2}$ values are listed in Table 3. Consistent with the in vitro modification results, co-injection of H-Ras and analogues **4**−**9** results in maturation of the oocytes, while co-injection of H-Ras and analogues *o*-CF_3O-AGPP **3**, *p*-NO_2-AGPP **10**, *p*-CN-AGPP **11**, and Isox-GPP **12** failed to promote maturation. Interestingly, *p*-Br-AGPP analogue **8** promotes oocyte maturation approximately as effectively as GPP **2**, analogues **4**−**6**, and AGPP **9**. *m*-Ethyl-AGPP **7** is the only FPP analogue that shows a significant increase in the maturation $t_{1/2}$ upon co-injection with H-Ras. On the other hand, co-injection of H-Ras with *m*-iodo-AGPP **6** slightly increased the rate of oocyte maturation compared to that of the premodified protein. The same $t_{1/2}$ was determined for H-Ras co-injected with FPP and with *m*-iodo-AGPP **6**. None of the analogues accelerated the maturation of the oocytes relative to farnesylated H-Ras. These findings indicate that the *X. laevis* FTase is able to transfer FPP analogues **4**−**9** to H-Ras in situ. However, these results suggest that *m*-Et-AGPP **7** is a poor substrate for *X. laevis* FTase-catalyzed transfer to H-Ras. With the exception of *m*-Et-AGPP **7**, it appears that the rate of in situ FTase-catalyzed modification of H-Ras by the analogues was not rate-limiting for oocyte maturation. In the cases of analogues *o*-CF_3O-AGPP **3**, *p*-NO_2-AGPP **10**, *p*-CN-AGPP **11**, and Isox-GPP **12**, because no maturation was observed, it was not possible to determine if the *X. laevis* FTase was able to transfer analogues to co-injected H-Ras.

Analogue-Dependent Delayed Maturation Correlates with MAPK Activation. Oncogenic H-Ras stimulates the MAPK cascade in *Xenopus* ooctyes (*54*, *55*), and MAPK is necessary for H-Ras-induced GVBD (*53*, *56*). Microinjection of unlipidated oncogenic H-Ras into lovastatin-treated oocytes fails to activate MAPK as isoprenylation is prevented. Further, progesterone activates MAPK and stimulates subsequent GVBD in isoprenoid-depleted oocytes in an H-Ras-independent fashion. MAPK is essential for regulation of the cell cycle in oocytes and is a critical point at which H-Ras and progesterone signaling converge (*53*). The results from the microinjection experiments described above suggest that analogues **4**−**9** are functional farnesyl group replacements since they support GVBD while analogues *p*-NO_2-AGPP **10**, *p*-CN-AGPP **11**, and Isox-GPP **12** are RFIs. We therefore assayed MAPK activation in oocytes co-injected with activated H-Ras and the substituted anilinogeranyl diphosphates (Figure 5). We found that MAPK activation preceded GVBD upon co-injection of H-Ras and FPP or analogues **4**−**9** into lovastatin-treated oocytes, and that MAPK was not

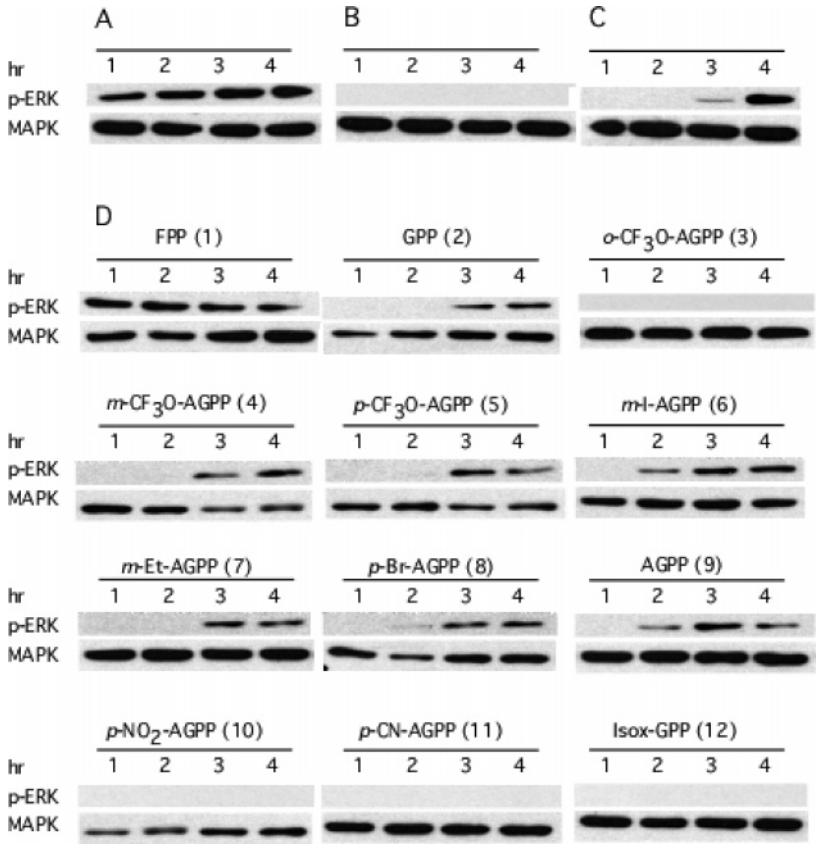

FIGURE 5: H-Ras co-injected with analogues **10**−**12** fails to activate MAPK in *Xenopus* oocytes. The time course of MAPK activation was evaluated by detecting the appearance of p-ERK in stage V or VI oocytes treated as described below. Lysates from lanes with 0.1 oocyte equivalent were separated by SDS−PAGE and subjected to Western blot analysis using either anti-p-ERK (top) or anti-MAPK/ERK1/2-CT (bottom) antibodies. (A) Oocytes were microinjected with 5 pmol of H-Ras as a positive control. (B) Oocytes were incubated with lovastatin for 16 h and then microinjected with 5 pmol of H-Ras as a negative control. (C) Oocytes were incubated with lovastatin for 16 h and then microinjected with 5 pmol of H-Ras followed by treatment with 10 μM progesterone as a positive control. (D) Oocytes were incubated with lovastatin for 16 h and then microinjected with 5 pmol of H-Ras each and the indicated isoprenoid diphosphates. Representative data from at least three independent assays are shown.

activated when RFIs *p*-NO_2-AGPP **10**, *p*-CN-AGPP **11**, and Isox-GPP **12** or the nontransferrable analogue *o*-CF_3O-AGPP **3** was employed.

Microinjection of oncogenic H-Ras into untreated oocytes or co-injection of H-Ras and FPP into lovastatin-treated oocytes results in activation of MAPK within 1 h. MAPK activation was delayed relative to FPP for all of the analogues that stimulated GVBD. Activated MAPK was not detected until the 2 h time point for *m*-I-AGPP **6**, *p*-Br-AGPP **8**, and AGPP **9**. For *m*-CF_3O-AGPP **4**, *p*-CF_3O-AGPP **5**, *m*-Et-AGPP **7**, and GPP **2**, the appearance of activated MAPK was delayed until the 3 h time point. Interestingly, MAPK activation for *m*-Et-AGPP **7** follows the same time course as *m*-CF_3O-AGPP **4**, *p*-CF_3O-AGPP **5**, and GPP **2** even though GVBD is substantially delayed with respect to these analogues in co-injection experiments (Table 1). As expected, in oocytes stimulated with progesterone, MAPK was activated regardless of lovastatin treatment. These data suggest that the delays in, or the absence of, GVBD are the result of delayed or absent MAPK activation downstream of H-Ras. Taken together, these data indicate that the defect in oocyte maturation is downstream of the three post-translational processing steps that lead to a mature C-terminus of H-Ras and that appearance of the defect is correlated with the reduced hydrophobicity of the prenyl lipid.

Anilinogeranyl Diphosphates Are Unable To Stimulate GVBD in the Absence of H-Ras and Are Not Acutely Toxic to X. laevis Oocytes. Our results for the analogues support the view that modification of H-Ras by a prenyl group or hydrophobic prenyl analogue is a necessary but not sufficient condition for oocyte maturation (*37*). However, it was possible that some of the analogues might be able to stimulate GVBD in a manner independent of H-Ras. An additional concern was that analogues *p*-NO_2-AGPP **10**, *p*-CN-AGPP **11**, and Isox-GPP **12** may be toxic and interfere with MAPK activation and GVBD induction by the in vitro and in situ modified H-Ras. To address these points, 12.5 pmol of compounds **1**−**12** was microinjected into lovastatin-treated oocytes in the absence of activated H-Ras. This concentration is 2.5-fold higher than that used in the experiments described above, to maximize any potential signaling activity or toxicity. With the exception of a single oocyte injected with GPP **2**, none of the compounds were able to induce GVBD over the 24 h period postinjection (data not shown). However, subsequent treatment with 10 μM progesterone stimulated GVBD in all of the analogue-injected oocytes. Compared with control or when FPP was injected, there is no statistically significant difference in the total number of oocytes that underwent GVBD. These data suggest that the analogues are not cytotoxic at the concentrations used over the time period of the experiment. More importantly, because progesterone-stimulated maturation proceeds normally, the analogues do not substantially interfere with the MAPK signaling cascade downstream from H-Ras.

DISCUSSION

Our studies demonstrate that FTase-transferrable FPP analogues with logP values of ≤3.1 can act as H-Ras function inhibitors (RFIs). Specifically, analogues *p*-NO_2-AGPP **10**, *p*-CN-AGPP **11**, and Isox-GPP **12** blocked H-Ras function, despite being efficiently transferred by FTase and processed by Rce1 and Icmt in vitro. The simplest explanation for these data is that a minimum lipophilicity of the prenyl group is necessary to allow important downstream interactions of the fully C-terminally processed H-Ras. Consistent with the observations of Dudler and Gelb (*37*), we find that GPP **2** is inefficiently transferred to H-Ras and poorly processed by Rce1 and/or Icmt in vitro, preventing efficient targeting of H-Ras to the proper cellular membranes. In contrast, analogues **4**−**12** are efficiently transferred to H-Ras, and analogues AGPP **9**, *p*-NO_2-AGPP **10**, *p*-CN-AGPP **11**, and Isox-GPP **12** support processing by both Rce1 and Icmt in a manner similar to that of FPP **1**. Importantly, the anilinogeranyl analogues exhibit no apparent cytotoxicity in *Xenopus* oocytes and were, by themselves, unable to stimulate GVBD. In contrast to FTIs, which inhibit FTase, RFIs are prenyl analogues that are efficiently transferred by FTase to H-Ras proteins whose signaling functions are then blocked. In light of this, our results may have important implications for the development of RFIs as potential alternatives to FTIs.

ACKNOWLEDGMENT

We thank Dr. Carol Fierke, Heather Hartman, Katherine Hicks, and Jennifer Pickett for the gift of mammalian protein farnesyl transferase.

SUPPORTING INFORMATION AVAILABLE

Detailed experimental procedure and spectroscopic data for compounds **6**, **7**, **11**, and **12**. This material is available free of charge via the Internet at http://pubs.acs.org.

REFERENCES

1. Adjei, A. A. (2003) An overview of farnesyltransferase inhibitors and their role in lung cancer therapy, *Lung Cancer 41* (Suppl. 1), S55−S62.
2. Rowinsky, E. K., Windle, J. J., and Von Hoff, D. D. (1999) Ras protein farnesyltransferase: A strategic target for anticancer therapeutic development, *J. Clin. Oncol. 17*, 3631−3652.
3. Zhu, K., Hamilton, A. D., and Sebti, S. M. (2003) Farnesyltransferase inhibitors as anticancer agents: Current status, *Curr. Opin. Invest. Drugs 4*, 1428−1435.
4. Zhang, F. L., and Casey, P. J. (1996) Protein prenylation: Molecular mechanisms and functional consequences, *Annu. Rev. Biochem. 65*, 241−269.
5. Vergnes, L., Peterfy, M., Bergo, M. O., Young, S. G., and Reue, K. (2004) Lamin B1 is required for mouse development and nuclear integrity, *Proc. Natl. Acad. Sci. U.S.A. 101*, 10428−10433.
6. Moores, S. L., Schaber, M. D., Mosser, S. D., Rands, E., O'Hara, M. B., Garsky, V. M., Marshall, M. S., Pompliano, D. L., and Gibbs, J. B. (1991) Sequence dependence of protein isoprenylation, *J. Biol. Chem. 266*, 14603−14610.
7. Roskoski, R., Jr. (2003) Protein prenylation: A pivotal posttranslational process, *Biochem. Biophys. Res. Commun. 303*, 1−7.
8. Dunten, P., Kammlott, U., Crowther, R., Weber, D., Palermo, R., and Birktoft, J. (1998) Protein Farnesyltransferase: Structure and Implications for Substrate Binding, *Biochemistry 37*, 7907−7912.
9. Caplin, B. E., Ohya, Y., and Marshall, M. S. (1998) Amino acid residues that define both the isoprenoid and CAAX preferences of the *Saccharomyces cerevisiae* protein farnesyltransferase. Creating the perfect farnesyltransferase, *J. Biol. Chem. 273*, 9472−9479.
10. Adjei, A. A. (2001) Blocking oncogenic Ras signaling for cancer therapy, *J. Natl. Cancer Inst. 93*, 1062−1074.
11. Ramamurthy, V., Roberts, M., van den Akker, F., Niemi, G., Reh, T. A., and Hurley, J. B. (2003) AIPL1, a protein implicated in Leber's congenital amaurosis, interacts with and aids in processing of farnesylated proteins, *Proc. Natl. Acad. Sci. U.S.A. 100*, 12630−12635.
12. Scheffzek, K., Stephan, I., Jensen, O. N., Illenberger, D., and Gierschik, P. (2000) The Rac−RhoGDI complex and the structural basis for the regulation of Rho proteins by RhoGDI, *Nat. Struct. Biol. 7*, 122−126.
13. Chen, X., Yano, Y., Hasuma, T., Yoshimata, T., Yinna, W., and Otani, S. (1999) Inhibition of farnesyl protein transferase and P21ras memebrane association by D-limonene in human pancreas tumor cells in vitro, *Chin. Med. Sci. J. 14*, 138−144.
14. Otto, J. C., Kim, E., Young, S. G., and Casey, P. J. (1999) Cloning and characterization of a mammalian prenyl protein-specific protease, *J. Biol. Chem. 274*, 8379−8382.
15. Bergo, M. O., Gavino, B. J., Hong, C., Beigneux, A. P., McMahon, M., Casey, P. J., and Young, S. G. (2004) Inactivation of Icmt inhibits transformation by oncogenic K-Ras and B-Raf, *J. Clin. Invest. 113*, 539−550.
16. Michaelson, D., Ali, W., Chiu, V. K., Bergo, M., Silletti, J., Wright, L., Young, S. G., and Philips, M. (2005) Postprenylation CAAX Processing Is Required for Proper Localization of Ras but Not Rho GTPases, *Mol. Biol. Cell 16*, 1606−1616.
17. Fujiyama, A., Tsunasawa, S., Tamanoi, F., and Sakiyama, F. (1991) S-Farnesylation and methyl esterification of C-terminal domain of yeast RAS2 protein prior to fatty acid acylation, *J. Biol. Chem. 266*, 17926−17931.
18. Resh, M. D. (2004) Membrane targeting of lipid modified signal transduction proteins, *Subcell. Biochem. 37*, 217−232.
19. Russo, P., Loprevite, M., Cesario, A., and Ardizzoni, A. (2004) Farnesylated proteins as anticancer drug targets: From laboratory to the clinic, *Curr. Med. Chem.: Anti-Cancer Agents 4*, 123−138.
20. Anwar, K., Nakakuki, K., Shiraishi, T., Naiki, H., Yatani, R., and Inuzuka, M. (1992) Presence of ras oncogene mutations and human papillomavirus DNA in human prostate carcinomas, *Cancer Res. 52*, 5991−5996.
21. Watanabe, M., Shiraishi, T., Yatani, R., Nomura, A. M., and Stemmermann, G. N. (1994) International comparison on ras gene mutations in latent prostate carcinoma, *Int. J. Cancer 58*, 174−178.
22. Konishi, N., Hiasa, Y., Matsuda, H., Tao, M., Tsuzuki, T., Hayashi, I., Kitahori, Y., Shiraishi, T., Yatani, R., Shimazaki, J., et al. (1995) Intratumor cellular heterogeneity and alterations in ras oncogene and p53 tumor suppressor gene in human prostate carcinoma, *Am. J. Pathol. 147*, 1112−1122.
23. Santucci, R., Mackley, P. A., Sebti, S., and Alsina, M. (2003) Farnesyltransferase inhibitors and their role in the treatment of multiple myeloma, *Cancer Control 10*, 384−387.
24. Sebti, S. M., and Hamilton, A. D. (2000) Farnesyltransferase and geranylgeranyltransferase I inhibitors in cancer therapy: Important mechanistic and bench to bedside issues, *Expert Opin. Invest. Drugs 9*, 2767−2782.
25. Reid, T. S., and Beese, L. S. (2004) Crystal structures of the anticancer clinical candidates R115777 (Tipifarnib) and BMS-214662 complexed with protein farnesyltransferase suggest a mechanism of FTI selectivity, *Biochemistry 43*, 6877−6884.
26. Cox, A. D. (2001) Farnesyltransferase inhibitors: Potential role in the treatment of cancer, *Drugs 61*, 723−732.
27. Fiordalisi, J. J., Johnson, R. L., II, Weinbaum, C. A., Sakabe, K., Chen, Z., Casey, P. J., and Cox, A. D. (2003) High affinity for farnesyltransferase and alternative prenylation contribute individually to K-Ras4B resistance to farnesyltransferase inhibitors, *J. Biol. Chem. 278*, 41718−41727.
28. Crespo, N. C., Ohkanda, J., Yen, T. J., Hamilton, A. D., and Sebti, S. M. (2001) The farnesyltransferase inhibitor, FTI-2153, blocks bipolar spindle formation and chromosome alignment and causes prometaphase accumulation during mitosis of human lung cancer cells, *J. Biol. Chem. 276*, 16161−16167.
29. Ashar, H. R., James, L., Gray, K., Carr, D., Black, S., Armstrong, L., Bishop, W. R., and Kirschmeier, P. (2000) Farnesyl transferase inhibitors block the farnesylation of CENP-E and CENP-F and

alter the association of CENP-E with the microtubules, *J. Biol. Chem. 275*, 30451−30457.
30. Cox, A. D., and Der, C. J. (1992) Protein prenylation: More than just glue? *Curr. Opin. Cell Biol. 4*, 1008−1016.
31. Dudler, T., and Gelb, M. H. (1996) Palmitoylation of Ha-Ras facilitates membrane binding, activation of downstream effectors, and meiotic maturation in *Xenopus* oocytes, *J. Biol. Chem. 271*, 11541−11547.
32. Dolence, E. K., Dolence, J. M., and Poulter, C. D. (2000) Solid-Phase Synthesis of a Farnesylated CaaX Peptide Library: Inhibitors of the Ras CaaX Endoprotease, *J. Comb. Chem. 2*, 522−536.
33. Dolence, J. M., Steward, L. E., Dolence, E. K., Wong, D. H., and Poulter, C. D. (2000) Studies with Recombinant *Saccharomyces cerevisiae* CaaX Prenyl Protease Rce1p, *Biochemistry 39*, 4096−4104.
34. Graham, S. L., deSolms, S. J., Giuliani, E. A., Kohl, N. E., Mosser, S. D., Oliff, A. I., Pompliano, D. L., Rands, E., Breslin, M. J., Deana, A. A., et al. (1994) Pseudopeptide inhibitors of Ras farnesyl-protein transferase, *J. Med. Chem. 37*, 725−732.
35. Lerner, E. C., Qian, Y., Blaskovich, M. A., Fossum, R. D., Vogt, A., Sun, J., Cox, A. D., Der, C. J., Hamilton, A. D., and Sebti, S. M. (1995) Ras CAAX peptidomimetic FTI-277 selectively blocks oncogenic Ras signaling by inducing cytoplasmic accumulation of inactive Ras-Raf complexes, *J. Biol. Chem. 270*, 26802−26806.
36. Gibbs, J. B., Pompliano, D. L., Mosser, S. D., Rands, E., Lingham, R. B., Singh, S. B., Scolnick, E. M., Kohl, N. E., and Oliff, A. (1993) Selective inhibition of farnesyl-protein transferase blocks ras processing in vivo, *J. Biol. Chem. 268*, 7617−7620.
37. Dudler, T., and Gelb, M. H. (1997) Replacement of the H-Ras Farnesyl Group by Lipid Analogues: Implications for Downstream Processing and Effector Activation in *Xenopus* Oocytes, *Biochemistry 36*, 12434−12441.
38. Gibbs, B. S., Zahn, T. J., Mu, Y., Sebolt-Leopold, J. S., and Gibbs, R. A. (1999) Novel Farnesol and Geranylgeraniol Analogues: A Potential New Class of Anticancer Agents Directed against Protein Prenylation, *J. Med. Chem. 42*, 3800−3808.
39. McGeady, P., Kuroda, S., Shimizu, K., Takai, Y., and Gelb, M. H. (1995) The farnesyl group of H-Ras facilitates the activation of a soluble upstream activator of mitogen-activated protein kinase, *J. Biol. Chem. 270*, 26347−26351.
40. Zhao, J., Kung, H. F., and Manne, V. (1994) Farnesylation of p21 Ras proteins in *Xenopus* oocytes, *Cell. Mol. Biol. Res. 40*, 313−321.
41. Dudler, T., and Gelb, M. H. (1999) Probing the role of H-Ras lipidation for signaling functions in *Xenopus laevis* oocytes, *Methods Mol. Biol. 116*, 161−176.
42. Subramanian, T., Wang, Z., Troutman, J. M., Andres, D. A., and Spielmann, H. P. (2005) Directed library of anilinogeranyl analogues of farnesyl diphosphate via mixed solid- and solution-phase synthesis, *Org. Lett. 7*, 2109−2112.
43. Chehade, K. A., Andres, D. A., Morimoto, H., and Spielmann, H. P. (2000) Design and synthesis of a transferable farnesyl pyrophosphate analogue to Ras by protein farnesyltransferase, *J. Org. Chem. 65*, 3027−3033.
44. Davisson, V. J., Woodside, A. B., and Poulter, C. D. (1985) Synthesis of allylic and homoallylic isoprenoid pyrophosphates, *Methods Enzymol. 110*, 130−144.
45. Pompliano, D. L., Gomez, R. P., and Anthony, N. J. (1992) Intramolecular Fluorescence Enhancement: A Continuous Assay of Ras Farnesyl-Protein Transferase, *J. Am. Chem. Soc. 114*, 7945−7946.
46. Lambert, W. J. (1993) Modeling Oil-Water Partitioning and Membrane Permeation Using Reversed-Phase Chromatography, *J. Chromatogr., A 656*, 469−484.
47. Niemi, R., Vepsalainen, J., Taipale, H., and Jarvinen, T. (1999) Bisphosphonate prodrugs: Synthesis and in vitro evaluation of novel acyloxyalkyl esters of clodronic acid, *J. Med. Chem. 42*, 5053−5058.
48. *Sybyl* (2004) Tripos, Inc., St. Louis, MO.
49. Gasteiger, J., and Marsili, M. (1980) Iterative Partial Equalization of Orbital Electronegativity: A Rapid Access to Atomic Charges, *Tetrahedron 36*, 3219−3228.
50. *WebLab Viewpro* (2000) Accelrys Software Inc., San Diego, CA.
51. Andres, D. A., Shao, H., Crick, D. C., and Finlin, B. S. (1997) Expression cloning of a novel farnesylated protein, RDJ2, encoding a DnaJ protein homologue, *Arch. Biochem. Biophys. 346*, 113−124.
52. Chehade, K. A., Kiegiel, K., Isaacs, R. J., Pickett, J. S., Bowers, K. E., Fierke, C. A., Andres, D. A., and Spielmann, H. P. (2002) Photoaffinity analogues of farnesyl pyrophosphate transferable by protein farnesyl transferase, *J. Am. Chem. Soc. 124*, 8206−8219.
53. Carnero, A., Jimenez, B., and Lacal, J. C. (1994) Progesterone but not ras requires MPF for in vivo activation of MAPK and S6 KII: MAPK is an essential conexion point of both signaling pathways, *J. Cell. Biochem. 55*, 465−476.
54. Hattori, S., Fukuda, M., Yamashita, T., Nakamura, S., Gotoh, Y., and Nishida, E. (1992) Activation of mitogen-activated protein kinase and its activator by ras in intact cells and in a cell-free system, *J. Biol. Chem. 267*, 20346−20351.
55. Pomerance, M., Schweighoffer, F., Tocque, B., and Pierre, M. (1992) Stimulation of mitogen-activated protein kinase by oncogenic Ras p21 in *Xenopus* oocytes. Requirement for Ras p21-GTPase-activating protein interaction, *J. Biol. Chem. 267*, 16155−16160.
56. Kosako, H., Gotoh, Y., and Nishida, E. (1994) Requirement for the MAP kinase kinase/MAP kinase cascade in *Xenopus* oocyte maturation, *EMBO J. 13*, 2131−2138.

BI061704+